

This discussion paper is/has been under review for the journal *Atmospheric Chemistry and Physics (ACP)*. Please refer to the corresponding final paper in *ACP* if available.

**Inverse modeling of
European CH₄
emissions**

M. G. Villani et al.

Inverse modeling of European CH₄ emissions: sensitivity to the observational network

M. G. Villani¹, P. Bergamaschi¹, M. Krol^{2,3,4}, J. F. Meirink⁵, and F. Dentener¹

¹European Commission, Joint Research Centre, Institute for Environment and Sustainability, 21027 Ispra (VA), Italy

²Wageningen University and Research Centre, Wageningen, The Netherlands

³Institute for Marine and Atmospheric Research Utrecht (IMAU), Utrecht, The Netherlands

⁴SRON Netherlands Institute for Space Research, Utrecht, The Netherlands

⁵Royal Netherlands Meteorological Institute, De Bilt, The Netherlands

Received: 19 August 2009 – Accepted: 13 September 2009 – Published: 6 October 2009

Correspondence to: M. G. Villani (mgvillani@gmail.com)

Published by Copernicus Publications on behalf of the European Geosciences Union.

Title Page

Abstract

Introduction

Conclusions

References

Tables

Figures

◀

▶

◀

▶

Back

Close

Full Screen / Esc

Printer-friendly Version

Interactive Discussion



Abstract

Inverse modeling is widely employed to provide “top-down” emission estimates using atmospheric measurements. Here, we analyze the dependence of derived CH₄ emissions on the sampling frequency and density of the observational surface network, using the TM5-4DVAR inverse modeling system and synthetic observations. This sensitivity study focuses on Europe.

The synthetic observations are created by TM5 forward model simulations. The inversions of these synthetic observations are performed using virtually no knowledge on the *a priori* spatial and temporal distribution of emissions, i.e. the emissions are derived mainly from the atmospheric signal detected by the measurement network.

Using the European network of stations for which continuous or weekly flask measurements are available for 2001, the synthetic experiments can retrieve the “true” annual total emissions for single countries such as France within 20%, and for all North West European countries together within ~5%. However, larger deviations are obtained for South and East European countries due to the scarcity of stations in the measurement network. Upgrading flask sites to stations with continuous measurements leads to an improvement for central Europe in emission estimates. For realistic emission estimates over the whole European domain, however, a major extension of the number of stations in the existing network is required. We demonstrate the potential of an extended network of a total of ~60 European stations to provide realistic emission estimates over the whole European domain.

1 Introduction

Inverse modeling of atmospheric CH₄ provides “top-down” emission estimates, and represents an important tool to analyze the global CH₄ budget (Bergamaschi et al., 2009; Chen and Prinn, 2006; Bousquet et al., 2005; Mikaloff Fletcher et al., 2004a, b; Houweling et al., 1999; Hein et al., 1997). In recent years, inverse modeling ef-

Inverse modeling of European CH₄ emissions

M. G. Villani et al.

Title Page

Abstract

Introduction

Conclusions

References

Tables

Figures



Back

Close

Full Screen / Esc

Printer-friendly Version

Interactive Discussion



forts have been extended also to the regional scale (e.g. on the spatial scales of single countries), using high-resolution models and better coverage of measurements (Bergamaschi et al., 2005; Manning et al., 2005). Such regional top-down estimates can be potentially used for verification of international agreements on emission reductions, such as the Kyoto protocol, which however requires constant monitoring in a dense network (Bergamaschi, 2007a; IPCC, 2000).

The four-dimensional variational inverse modeling system TM5-4DVAR, based on the atmospheric transport model TM5 (Krol et al., 2005), is designed to infer emissions from atmospheric observations. In particular, it allows optimizing emissions at the model grid cell scale (compared to optimization of larger geographical regions in previously used synthesis inversions). At the same time, large observational data sets can be used, such as high frequency in situ measurements, providing constraints on monthly emissions from concentration variations at synoptic time scales.

The TM5-4DVAR system as currently implemented (Bergamaschi et al., 2009; Meirink et al., 2008a, b) can be simultaneously applied to both surface observations and satellite based measurements made by sensors such as SCIAMACHY (Scanning Imaging Absorption Spectrometer for Atmospheric CHartographY) on ENVISAT. The existing surface stations are monitoring mainly the atmospheric background concentrations of greenhouse gases (such as the NOAA/CMDL, and AGAGE networks, e.g. Dlugokencky et al., 2003; Dlugokencky et al., 1994; Prinn et al., 1990), and have in recent years been extended to more regional stations (especially over Europe and North America). Nevertheless, the surface monitoring network is still sparse. The additional inclusion of satellite data from SCIAMACHY was recently reported in several studies (Bergamaschi et al., 2009; Meirink et al., 2008b; Frankenberg et al., 2008). While satellite data provide almost a global coverage of the methane concentration distribution, surface observations remain essential due to their higher accuracy and better temporal resolution for continuous in-situ measurements.

In this work we investigate the information content available from ground-based measurement observational networks. We will explore the sensitivity of the emissions de-

Inverse modeling of European CH₄ emissions

M. G. Villani et al.

[Title Page](#)[Abstract](#)[Introduction](#)[Conclusions](#)[References](#)[Tables](#)[Figures](#)[⏪](#)[⏩](#)[◀](#)[▶](#)[Back](#)[Close](#)[Full Screen / Esc](#)[Printer-friendly Version](#)[Interactive Discussion](#)

rived from the TM5-4DVAR system to the observational networks. The zooming capability of the TM5-4DVAR system gives the opportunity to better spatially resolve a specific domain, in a consistent global inversion framework. Here, the focus is on observational network in the European domain.

5 Several studies have already addressed the impact of the observational network on inversion results in inverse modeling approaches for GHG gases, based on synthesis inversions or mass balance approaches and focusing mainly on continental scale aggregated regions (e.g. Law et al., 2002, 2003, 2004; Law and Vohralik, 2001; Rayner et al., 1996). Only recently, first sensitivity studies have been presented also for the regional scales (e.g. Carouge et al., 2008a, b).

10 To test the sensitivity of our inverse modeling framework, we present experiments that use synthetic observations, similar to observing system simulation experiments (OSSEs) (e.g. Carouge et al., 2008a, b; Meirink et al., 2006; Chevallier, 2007). The advantage of this approach is that the generation of pseudo observations allows us to test the accuracy of the solution and the impact of different assumptions made on the network by direct comparisons of the derived CH₄ emissions to the ‘true’ emissions that were used to generate the pseudo-data. Given this simple setting where observations are generated with the same model used for the inversion, we do not expect this study to provide results directly applicable to real cases, but we can gain knowledge on the limits and potential of our model framework.

20 The goal of this study is to (i) analyze the information content of single measurement stations, and (ii) investigate the effect of different observational networks on the retrieved emissions, i.e. flask versus continuous sampling, and the size of the network. Our overall aim is to gain insight in the accuracy at which emissions can be derived at the country scale in Europe, and how this accuracy depends on the network properties.

**Inverse modeling of
European CH₄
emissions**

M. G. Villani et al.

Title Page

Abstract

Introduction

Conclusions

References

Tables

Figures

◀

▶

◀

▶

Back

Close

Full Screen / Esc

Printer-friendly Version

Interactive Discussion



2 Methodology

2.1 Synthetic observations

2.1.1 TM5 forward runs

Synthetic observations are generated by TM5 forward simulations. TM5 is a global of-
5 fline chemistry–transport model (Krol et al., 2005), driven by meteorological fields (6-h
forecasts) from the European Centre for Medium Range Weather Forecasts (ECMWF)
operational Integrated Forecast System (IFS). Key processes simulated in TM5 include
mass-conserving tracer advection, convection, and boundary layer mixing. TM5 has a
two-way nested zooming capability, which allows the model to perform higher horizon-
10 tal resolution simulations in specified $3^\circ \times 2^\circ$ and $1^\circ \times 1^\circ$ nested grids, embedded in the
global domain. In this study, TM5 is run on a regular grid with horizontal resolution of
 $6^\circ \times 4^\circ$ globally, and two embedded zoom regions of $3^\circ \times 2^\circ$ and $1^\circ \times 1^\circ$ degree resolution
over Europe (Fig. 1). In the vertical direction, 25 layers are used, defined as a subset
of the 60 layers used operationally in the ECMWF IFS model until 2006.

15 We apply the CH_4 tracer version as described in Bergamaschi et al. (2009). Chem-
ical destruction of CH_4 by OH radicals in the troposphere is simulated using pre-
calculated OH fields based on Carbon Bond Mechanism 4 (CBM-4) chemistry and
optimized with methyl chloroform (Bergamaschi et al., 2005; Houweling et al., 1998).
Chemical destruction of CH_4 by OH, Cl, and $\text{O}(^1\text{D})$ in the stratosphere is based on the
20 2-D photochemical Max-Planck-Institute (MPI) model (Brühl and Crutzen, 1993).

The emission inventories used in the TM5 forward runs represent in our experiments
the “true” emissions, applied to generate the pseudo observations. The emissions are
based on current “state-of-the-art” bottom-up inventories as used in Bergamaschi et
al. (2009) (see Table 1), and include the major CH_4 natural and anthropogenic source
25 categories. Emissions from wetlands, rice paddies, and biomass burning have sea-
sonal variations, while the emissions from all other source categories are assumed to
be constant. Over the European domain, anthropogenic emissions from ruminants,

Inverse modeling of European CH_4 emissions

M. G. Villani et al.

Title Page

Abstract

Introduction

Conclusions

References

Tables

Figures

◀

▶

◀

▶

Back

Close

Full Screen / Esc

Printer-friendly Version

Interactive Discussion



waste handling, and emissions related to fossil fuels (coal mining, oil and gas production and distribution) are important. For the Scandinavian countries emissions from wetlands also play a major role. The spatial distribution of total annual mean emissions is shown in Fig. 2. The emission distribution for Europe is shown in more detail in Fig. 2b. Note that the emission hot spots located in the North Sea are related to oil and gas production.

Global CH₄ mixing ratios at the start of the simulations (1 January 2001) have been initialized using 3-D fields from inversions constrained by real observations for 2000–2001.

To account for potential observation and modeling errors we add noise to our synthetic observations. For this purpose, we apply a random function with a magnitude of 50% of the estimated “model representativeness error”, which includes estimates of the impact of the subgrid-scale variability of emissions on simulated mixing ratios for stations in the boundary layer, and a 3 ppb measurement error (Bergamaschi et al., 2009). Close to emission sources, the subgrid-scale variability of emissions, based on the spatial concentration gradient calculated in the forward run, generally outweighs the measurement error. Systematic biases in the observations are not taken into account in this study.

2.1.2 Atmospheric networks

The synthetic observations are created for global and European monitoring stations for which real observations are available for the year 2001, 37 remote sites and 17 European stations (Fig. 1 and Table 2). These stations are denoted “current stations” (CS) and include sites at which flask samples are collected (at a typical sampling frequency ~1 per week), and sites with continuous measurements (with a time resolution of 1 h or better). Remote stations use flask samples. Of the 17 European stations there are 11 flask-sampled, and 6 continuously-sampled sites. We generate synthetic flask samples (weekly) and continuous measurements (hourly), accordingly.

In addition to the current station network (CS), we consider the following extensions

Inverse modeling of European CH₄ emissions

M. G. Villani et al.

Title Page

Abstract

Introduction

Conclusions

References

Tables

Figures

◀

▶

◀

▶

Back

Close

Full Screen / Esc

Printer-friendly Version

Interactive Discussion



of the network:

- (1) in a first upgrading step, the current 11 European flask sampling sites are converted into sites with continuous measurements (denoted “current stations continuous measurements”, CS-CM).
- (2) In a second step, further stations (50 sites in total) are added in Europe (denoted as “extended network”, EXT). These include 16 stations for which real measurements have started after 2001 (e.g. various tall towers from the CHIOTTO – Continuous High precision Tall Tower Observations of greenhouse gases-network) or have been recently proposed in research proposals. Additional 34 stations are added primarily in South and Eastern Europe to achieve a comprehensive coverage of the European domain. For simplicity, in many cases the latter stations are placed at the outskirts of major cities, when possible close to facilities such as airports or research centers. In the entirely synthetic framework of this study, this approach should be suitable to illustrate the potential benefits of such an extended network. However, these sites are not meant to evaluate the optimal locations and density of a network, neither to be concrete proposals for new stations. For the extension of the real network, many aspects have to be considered, such as the site representativeness of a larger region (e.g. absence of important local sources), requiring for each potential new site a detailed analysis of the region of influence.

The atmospheric stations used in this study are compiled in Table 2 and shown in Fig. 1.

2.2 TM5-4DVAR inverse modeling system

We employ the TM5-4DVAR inverse modeling system, based on the TM5 model and its adjoint (Krol et al., 2008), and a four-dimensional variational optimization technique. The main parts of the system are described in detail in Meirink et al. (2008a) and subsequent further improvements in Bergamaschi et al. (2009). Briefly, the TM5-4DVAR

Inverse modeling of European CH₄ emissions

M. G. Villani et al.

Title Page

Abstract

Introduction

Conclusions

References

Tables

Figures

◀

▶

◀

▶

Back

Close

Full Screen / Esc

Printer-friendly Version

Interactive Discussion



system is minimizing iteratively the cost function to find an optimal set of model parameters (control vector \mathbf{x}):

$$J(\mathbf{x}) = \frac{1}{2} (\mathbf{x} - \mathbf{x}_B)^T \mathbf{B}^{-1} (\mathbf{x} - \mathbf{x}_B) + \frac{1}{2} \sum_{i=1}^n (H_i(\mathbf{x}) - \mathbf{y}_{\text{OBS},i})^T \mathbf{R}_i^{-1} (H_i(\mathbf{x}) - \mathbf{y}_{\text{OBS},i}) \quad (1)$$

where \mathbf{x}_B is the *a priori* estimate of \mathbf{x} , and \mathbf{B} the parameter error covariance matrix (containing the uncertainties of the parameters and their correlations in space and time). The variable $\mathbf{y}_{\text{OBS},i}$ denotes the set of observational data at time i , \mathbf{R}_i their corresponding error covariance matrix, and $H_i(\mathbf{x})$ the simulated concentrations corresponding to the observations.

In our case, the control vector consists of monthly-mean surface emissions for each model grid cell, and the three-dimensional concentration field at the start of the inversion period. In contrast to inversions that apply detailed *a priori* emission inventories (e.g. Bergamaschi et al., 2009), and optimize different source categories independently, we optimize here only the total emissions for each grid cell.

The parameter error covariance matrix \mathbf{B} is split into spatial and temporal correlation matrices (Meirink et al., 2008a). Spatial correlations are modeled as Gaussian functions of the distance between grid cells, and temporal correlations as exponential functions of the time difference (for the emissions only). Vertical correlations of errors in the initial concentration field have been estimated using the National Meteorological Center (NMC) method as outlined in (Meirink et al., 2006).

In this study we apply a “semi-exponential” description of the probability density function (PDF) of *a priori* emission errors (Bergamaschi et al., 2009) to avoid negative *a posteriori* emissions. Due to the non-linearity of this “semi-exponential” approach a system with an outer loop for evaluation of the non-linear model and an inner loop for incremental optimization of the linearized model is used (for details see Bergamaschi et al., 2009). In a set of sensitivity experiments, we also evaluate the effect of using the “semi-exponential” PDF compared to a regular Gaussian PDF.

Inverse modeling of European CH₄ emissions

M. G. Villani et al.

[Title Page](#)[Abstract](#)[Introduction](#)[Conclusions](#)[References](#)[Tables](#)[Figures](#)[◀](#)[▶](#)[◀](#)[▶](#)[Back](#)[Close](#)[Full Screen / Esc](#)[Printer-friendly Version](#)[Interactive Discussion](#)

2.3 Inversion set-up

As a starting point of our inversions, we create an *a priori* emission inventory in which emissions are distributed homogeneously over land (except Antarctica), using an annual total of 500 Tg CH₄/yr. In addition, we account for a homogeneously distributed total of 17 Tg CH₄/yr over the ocean. A priori emissions on a global scale are shown in Fig. 2c. These homogeneous emissions are assumed to be constant in time. The *a priori* uncertainty of these emissions is set to large values (300% of the *a priori* grid-cell emissions). This is consistent with the value of the mean relative difference between true and *a priori* emissions over Europe at the grid-scale, which is about 200%. The spatial correlation length for the emissions is set to rather small values (50 km) to give the inverse modeling system a large degree of freedom to optimize the spatial emission patterns. A correlation length of 50 km implies that emissions in neighboring grid-cells are significantly correlated over areas as wide as large metropolitan and industrial locations. Emissions in neighboring grid-cells are correlated with correlation coefficients (values of the **B** matrix described in Sect. 2.1) equal to 0.6, on average in Europe. These values vary according to the latitude, e.g. about 0.80 at 60° N and 0.40 for 32° N. Furthermore, we assume a temporal error correlation time of one month. The inversions are run over a 12-month period (from 1 January 2001 until 1 January 2002), during which the monthly emissions are optimized. Each inversion, performed at a single processor of IBM Power 5 cluster at the European Centre for Medium-Range Weather Forecasts (ECMWF), requires approximately 20 days of computational time.

We apply here the same sampling scheme for the atmospheric observations as in the previous inversions described by Bergamaschi et al. (2009). This implies that continuous measurements are sampled only once per day to avoid the continuous measurements to over-constrain the inversion. Stations in the boundary layer are generally sampled during daytime (from 12:00–15:00 h local time), while mountain stations are sampled during nighttime (from 00:00–03:00 h local time). This strategy avoids sampling in the shallow nighttime boundary layer and sampling during upslope transport

Inverse modeling of European CH₄ emissions

M. G. Villani et al.

Title Page

Abstract

Introduction

Conclusions

References

Tables

Figures

⏪

⏩

◀

▶

Back

Close

Full Screen / Esc

Printer-friendly Version

Interactive Discussion



for mountain stations.

The inversions are generally performed in two cycles. After a first inversion, we reject observations that differ by more than three sigmas (overall observational and model-representativeness error calculated during the inversion) from the *a posteriori* model simulation. In case of using true atmospheric observations, such large deviations are normally caused by the inability of the model to represent the observation (e.g. due to local emissions or local circulation processes). In the case of synthetic measurements, as used in this work, it means that if the sampling site is located in an area with large true emissions, the synthetic observations will show high concentrations and the perturbations to these observations can be potentially large. Since the homogeneous *a priori* emissions are much lower in these areas, the inversion may experience problems in reproducing these observations. If we do not perturb the observations, we would expect less discrepancy between modeled and observed data. In this case, we should also not reject any synthetic data as they all provide reliable information of the underlying emissions.

A second inversion cycle is performed using the reduced observational data set. The percentage of measurements that are rejected is generally less than 10%. The advantage of this two-step inversion should be seen in the light of “real world” inversion, where certain datasets cannot be represented by the model and need to be discarded.

2.4 Inversion experiments

The inversions performed in this study are compiled in Table 3.

To investigate the constraining effect of different station types, we perform inversions where only observations of a single European station are used (but maintaining the global background stations). We select (i) Mace Head (MHD, 25 m a.s.l.), a station which samples the marine background, but is also frequently influenced by air masses from the UK and Ireland, and partly also from continental Europe; (ii) the tall tower at Cabauw (CB4, 200 m a.s.l.), a typical boundary layer station; (iii) Schauinsland (SIL, 1205 m a.s.l.) a mountain station of medium altitude. We apply continuous

Inverse modeling of European CH₄ emissions

M. G. Villani et al.

Title Page

Abstract

Introduction

Conclusions

References

Tables

Figures

◀

▶

◀

▶

Back

Close

Full Screen / Esc

Printer-friendly Version

Interactive Discussion



observations for these single sites (but weekly flask samples for the global background stations). The three inversions are denoted I1, I2, and I3 for MHD, CB4 and SIL respectively (Table 3). In addition, we calculate directly the sensitivities of these three sites to emissions, using “back-plume” simulations based on the TM5 adjoint model (Krol et al., 2008).

In our main set of inversions (S1, S2, S3), we analyze the impact of the different observational networks on the retrieved emissions. As outlined in Sect. 2.1.2 these networks are denoted: S1 (current stations), S2 (current stations continuous measurements), and S3 (extended network).

For S1, we describe additional sensitivity experiments (scenarios S1.1, S1.2, S1.3, S1.4), in the Appendix. The aim of these experiments is to test the influence of the assumptions on *a priori* uncertainty and correlation length for the emissions (S1.1 and S1.2), and the impact of using perturbed synthetic observations in our TM5-4DVAR system (S1.3 and S1.4).

In Sect. 4.1 and 4.2, we present some additional sensitivity studies, S1a/b, S2a/b, and S3a/b, to investigate some bias encountered in inversions S1–S3. In these experiments the ocean emissions are set to zero, and both the semi-linear (a: using the semi-exponential PDF) and linear (b: using the regular Gaussian PDF) versions of the TM5-4DVAR system are applied. Furthermore, no perturbation of the synthetic observations is applied in these scenarios.

3 Results

3.1 Derived CH₄ emissions with inversion of single stations

We first analyze the potential of single stations to retrieve CH₄ emissions over Europe. Figure 3 shows the European annual mean CH₄ emission distributions resulting from the inversions (Fig. 3a, b, and c) together with footprints (Fig. 3d, e, and f) for single station back-plume simulations. The latter represent annual mean sensitivities of at-

Inverse modeling of European CH₄ emissions

M. G. Villani et al.

Title Page

Abstract

Introduction

Conclusions

References

Tables

Figures

◀

▶

◀

▶

Back

Close

Full Screen / Esc

Printer-friendly Version

Interactive Discussion



mospheric measurements to CH₄ emissions (similarly as described in Krol et al., 2008, with units in ppb/(kg/s)).

We observe that the inversions retain the *a priori* emission value over those European areas where the annual mean sensitivities are small. This suggests that air masses from these regions rarely reach the station location, and measurements at the specific site contain little information on emissions from areas with low calculated sensitivities.

Mace Head, MHD, a boundary layer/marine background station, has a footprint that covers mainly Ireland, the UK, and the upwind ocean sector. Furthermore, MHD is also partly sensitive to emissions from the north-west continental European region. We note that the single-station inversion wrongly assigns high emissions to areas southeast of the MHD station.

The Cabauw tall tower, CB4, a boundary layer station, has a strong sensitivity to emissions in a radius of ~300 km around the station. Therefore, areas of high emissions are reasonably well retrieved over the Benelux countries, and partly over the UK, France and Germany. Over Northern France, CH₄ emissions are somewhat overestimated in comparison to the true emissions.

Schauinsland, SIL, a mountain station at ~1200 m altitude, is less sensitive than Cabauw and Mace Head to regional emissions. It retrieves a quite homogenous emission pattern over Germany and Northern France, in line with the back-plume calculation. The Schauinsland station thus provides weak constraints on the regional scale, but could potentially provide emission information content for larger scales compared to what is detected by boundary layer stations (due to the smaller influence of local sources).

In our modeling framework, the results discussed before illustrate that the use of a single station is not sufficient to retrieve a reliable emission distribution over Europe, when little *a priori* knowledge on emissions is assumed.

Inverse modeling of European CH₄ emissions

M. G. Villani et al.

Title Page

Abstract

Introduction

Conclusions

References

Tables

Figures

◀

▶

◀

▶

Back

Close

Full Screen / Esc

Printer-friendly Version

Interactive Discussion



3.2 Derived CH₄ emissions from inversions with different observational networks

3.2.1 Scenarios S1, S2, and S3

Figure 4 shows the annual mean CH₄ emission distribution over Europe obtained from scenarios S1 (current stations), S2 (all current stations with continuous measurements), and S3 (extended network). The true emission distribution is shown in Fig. 4a. In addition, Fig. 5 and Table 4 report annual total CH₄ emissions calculated for several European countries.

The current observational network captures the spatial pattern of CH₄ emission distribution over Europe reasonably well, considering that the inversion was started with a uniform *a priori* distribution. CH₄ emissions are adequately retrieved from the UK, Ireland, France, Germany and the Benelux, hereafter named the North West European countries (NWE). In these countries, major hot-spots are retrieved (e.g. over Benelux and UK), consistently with the true distributions. Areas with high CH₄ emissions are also visible in Eastern Europe, on the borders of Poland, Czech Republic and Slovakia. However, they have a lower magnitude and are spread over larger areas.

The current network retrieves total emissions from the NWE countries within 5% of the true values (within 20% for single countries e.g. France). As we start from *a priori* emissions for the NWE sector that are 45% lower than the true values (Table 4), this demonstrates the strong constraints of the observations for the emissions of this sector.

Conversely, CH₄ emissions from Scandinavian regions (Norway, Sweden and Finland), Southern Europe (Italy in particular) and Eastern Europe (Poland) are not adequately captured. In some cases (e.g. Spain) retrieved methane emissions are close to the true values, but this is mainly because the homogeneous *a priori* emissions were already close to the true emission totals.

In scenario S2 (current stations continuous measurements), there is an improvement in the regional spatial patterns especially for the emission hot spot over Poland. Furthermore, in this scenario, the total emissions from the Scandinavian countries are

Inverse modeling of European CH₄ emissions

M. G. Villani et al.

Title Page

Abstract

Introduction

Conclusions

References

Tables

Figures

◀

▶

◀

▶

Back

Close

Full Screen / Esc

Printer-friendly Version

Interactive Discussion



better quantified. In Southern and Eastern Europe, however, CH₄ emissions are still poorly retrieved.

In scenario S3 (extended network), a major improvement of derived emissions is achieved, compared to S1 and S2. For the Scandinavian countries, country totals are closer to true values for Sweden (difference of less than 7%), and Finland (about 32%). In the UK and Germany, CH₄ emissions are retrieved to within about 7% and 2% difference, respectively. Major improvements are also seen especially in Eastern Europe (e.g. for Poland the difference between retrieved and true emissions is about 8%), and Southern Europe (e.g. Italy). However, there are also some countries (e.g. Norway, Denmark, and some Eastern European countries) for which derived total emissions are actually slightly worse than in scenario S2, with a positive bias of S3 compared to the true values. We will investigate these discrepancies further in Sect. 3.2.2.

To demonstrate the general improvement of the retrieved *a posteriori* methane emission pattern over land using an improved and extended network, we present in Table 5 the correlation coefficient (r) and the linear regression coefficients (offset and slope b) of the derived monthly CH₄ emissions versus the true values (e.g. more than 3000 data points). These values have been calculated considering the land pixels representing the “enlarged” EU27 Countries (EU27 with Norway, Switzerland, and former Yugoslavia), denoted here as En-EU27. Table 5 shows a substantial improvement in the correlation coefficients (0.47 for S1 and 0.74 for S3). Moreover, the offset is decreasing and the slope value gets closer to 1.

3.2.2 Sensitivity scenarios S1.1–S1.4

In the Appendix A1 and A2, we discuss the sensitivity of our results (for scenario S1) when we change the correlation length and the *a priori* errors in the emissions. Moreover, we analyze inversions where we used unperturbed pseudo observations (S1.3), and pseudo observations with smaller perturbations (S1.4). The results suggest that the choice of our experimental framework is rather robust regarding the choice of the correlation length (50 km) and the error on the *a priori* emissions (300%) (Scenar-

Inverse modeling of European CH₄ emissions

M. G. Villani et al.

Title Page

Abstract

Introduction

Conclusions

References

Tables

Figures

⏪

⏩

◀

▶

Back

Close

Full Screen / Esc

Printer-friendly Version

Interactive Discussion



ios S1.1, S1.2). Furthermore, from experiments S1.3 and S1.4 we conclude that our system is not very sensitive to the random perturbation of the pseudo observations.

However, there are several aspects of the *a posteriori* emission distributions calculated in scenarios S1, S2 and S3 that require further analyses:

1. All scenarios fail to retrieve the substantial CH₄ emissions from gas and oil production in the North Sea that are present in the true emission distribution (Fig. 4).
2. For some countries, the *a posteriori* annual total emissions of scenario S3 (our “best network”) appear to be biased high compared to the true value. The overestimate provided by S3 is often larger than for scenarios S1 and S2 (e.g. for En-EU27, scenario S3 provides annual total emissions overestimated by 11%; S2 by 7%, and S1 by 5%).
3. The *a posteriori* emissions in grid cells close to the station locations are in many cases biased high compared to the true emissions.

These issues will be discussed in the next sections.

4 Discussion

4.1 Emissions from the North Sea

In scenarios S1, S2 and S3, CH₄ emissions from the area over the North Sea, between the UK and the Scandinavian countries (located between 0° and 5° E, and 54° and 62° N, and denoted as “GBout” in Table 4) are not properly retrieved. This is mainly due to the very small *a priori* emissions over oceans, and partly to the lack of constraints over this region (there are no observational sites). As a result of the very small *a priori* emissions over oceans, the absolute *a priori* errors (chosen as 300% of the *a priori* emissions for both land and sea pixels) are relatively small. Therefore, the inversion system will be inclined to assign the emissions to the UK or the Scandinavian

Inverse modeling of European CH₄ emissions

M. G. Villani et al.

Title Page

Abstract

Introduction

Conclusions

References

Tables

Figures

◀

▶

◀

▶

Back

Close

Full Screen / Esc

Printer-friendly Version

Interactive Discussion



countries. This is confirmed by sensitivity experiments S1.a/b, S2.a/b, and S3.a/b, where the ocean emissions (including the oil and gas emissions in the North Sea) are removed from the true and *a priori* emission distributions. The next section discusses these scenarios in more detail.

4.2 Positive bias in scenario S3

Further experiments are conducted that can help to explain the positive bias for some countries using the highest density network. In these experiments, the ocean emissions (including oil and gas emissions over the North Sea) have been removed in the calculation of the pseudo-observations that are fed into the inversions. Furthermore, no perturbation of the synthetic observations is applied, i.e. overall more ideal settings are applied. For these scenarios, we stopped after the first inversion to avoid rejecting potentially important unperturbed observations (an issue also mentioned in Sect. 2.3).

In the first set of experiments (S1.a, S2.a, S3.a), we apply the semi-linear inversion of the TM5-4DVAR system (as for scenarios S1–S3). In the second set of experiments (S1.b, S2.b, S3.b) we use the linear version, i.e. with normally distributed *a priori* error pdf's.

In Fig. 5, annual totals of the *a posteriori* CH₄ emissions from S1.a, S2.a, and S3.a show lower emissions compared to S1–S3 for En-EU27 and in particular for Norway, Denmark, and the UK (Table 4). In each case the difference for En-EU27 (e.g. S3 versus S3.a) is approximately 0.5 Tg CH₄/yr, which roughly corresponds to the true value of the total annual anthropogenic CH₄ emissions over the North Sea in the offshore region (“GBout” in Table 4). This suggests that for scenarios S1, S2 and S3 the higher derived emissions from Scandinavian countries and UK are actually a result of the anthropogenic emissions from the North Sea that the TM5-4DVAR system cannot retrieve properly and erroneously attributes to the areas nearby the stations located at the coastlines (see also Sect. 4.3). Nevertheless, the *a posteriori* emissions (EU15, En-EU27) are still slightly overestimated in e.g. S3.a. Scenarios S1.b, S2.b, S3.b, generally show a much better agreement with the true emissions of the annual country

Inverse modeling of European CH₄ emissions

M. G. Villani et al.

Title Page

Abstract

Introduction

Conclusions

References

Tables

Figures

◀

▶

◀

▶

Back

Close

Full Screen / Esc

Printer-friendly Version

Interactive Discussion



totals (Fig. 5). This suggests that the semi-linear version of the TM5-4DVAR system introduces a small positive bias. The semi-linear version was introduced to suppress negative emissions in the *a posteriori* emissions and to suppress strong dipole structures (Bergamaschi et al., 2009). The semi-linear scheme employs a skewed emission probability density distribution (PDF) with smaller probabilities towards a zero emission. Emissions larger than the *a priori* value follow a normal Gaussian distribution. When the *a posteriori* emissions are aggregated to the country scale this assumption leads to a small positive bias of about 5% (based on the annual totals for En-EU27). The linear version indeed produces very pronounced dipole structures with negative emissions in the *a posteriori* emission distributions at the grid scale (not shown). These dipole structures cancel out when aggregated to country scale totals.

4.3 Retrieved emission hot-spots near measurement stations

Grid points close to boundary layer stations show a clear tendency to overestimate *a posteriori* emissions (e.g. for Cabauw in the Netherlands, London in the UK, Saclay in France, Quistello, and San Pietro Capofiume in the Po-valley). This feature becomes even clearer in the extended network. In the areas that are not covered by the current network, the additional stations cause higher *a posteriori* emissions in the grid cells close to the stations. One possible explanation is that homogeneous *a priori* emissions around these stations are often lower than the true emissions. The inversion system selects the most efficient way to match the pseudo observations. Thus, increasing the emissions in one grid box close to the station results in a lower perturbation of the background term of the cost function (Eq. 1) than enhancing emissions over larger areas. As shown in Fig. A1 a larger correlation length has the effect of reducing these artificial large emissions at some stations, but, as discussed in the Appendix A1, also smears out the retrieved peak values. The issue is currently investigated more closely. At the moment, we conclude that emissions retrieved on individual grid cells should not be over-interpreted. Retrieved emissions should always be analyzed at scales larger than a few grid cells.

Inverse modeling of European CH₄ emissions

M. G. Villani et al.

Title Page

Abstract

Introduction

Conclusions

References

Tables

Figures

◀

▶

◀

▶

Back

Close

Full Screen / Esc

Printer-friendly Version

Interactive Discussion



5 Conclusions

Using the current observational network of 17 European stations for which continuous or weekly flask measurements are available for 2001, our synthetic experiments show that the “true” annual total emissions from all North West European countries can be retrieved within ~5% (within 20% for single countries e.g. France), while larger deviations are obtained for South and East European countries due to the scarcity of stations in the measurement network. Upgrading the current flask sites to stations with continuous measurements improves the inversions, primarily for central Europe and some Scandinavian countries. However, for realistic emission estimates over the whole European domain, a much larger extension of the existing network is required. We demonstrate the potential of an extended network of a total of ~60 European stations to provide realistic emissions estimates over the whole European domain. We note that in this work we did not attempt to design an “optimal network”, which could derive realistic CH₄ emissions over the whole European domain also with less than 60 observational sites. We leave this investigation for future studies.

It is important to realize that with the current observational network we cannot retrieve emissions from Southern and Eastern European countries properly. In absence of observational sites, the knowledge of the *a priori* emission distribution becomes essential as the optimized emissions will remain close to the prescribed *a priori* distribution.

Finally, we investigated some important aspects of the TM5-4DVAR system.

- We demonstrated that continuous atmospheric observations provide strong constraints on emissions at regional scale, and allow deriving the major features of their spatial distributions. Increasing the network density markedly improves the agreement between retrieved and true emission patterns (clearly visible in the correlation coefficients). However, derived emissions of the individual model grid cells show major differences compared to the true emissions. In particular, we need to further investigate the overestimated emissions attributed to areas close

Inverse modeling of European CH₄ emissions

M. G. Villani et al.

Title Page

Abstract

Introduction

Conclusions

References

Tables

Figures

⏪

⏩

◀

▶

Back

Close

Full Screen / Esc

Printer-friendly Version

Interactive Discussion



Inverse modeling of European CH₄ emissions

M. G. Villani et al.

Title Page

Abstract

Introduction

Conclusions

References

Tables

Figures

◀

▶

◀

▶

Back

Close

Full Screen / Esc

Printer-friendly Version

Interactive Discussion



to boundary layer stations sampling in regions with high emissions.

- We did not use detailed *a priori* emission inventories for the inversions. Thus, we optimized emissions entirely from the atmospheric signal. The major *a priori* assumption in our model settings is that emissions are distributed mainly over land. While this assumption seems generally reasonable, it leads to some artifacts if large sources are located over the ocean. We showed that the system cannot retrieve the localized anthropogenic CH₄ emissions over the North Sea properly, and allocates them to the surrounding countries where observational sites are present.
- The semi-linear TM5-4DVAR version provides generally consistent emission patterns for the European countries. However, it also introduces a small positive bias (about 5% higher derived CH₄ emissions) compared to the linear version.
- We applied a large perturbation to our synthetic observations (50% of estimated representativeness error). However, since this perturbation was random, it had a relatively small effect on the derived country aggregated emissions. Future studies should also investigate the potential impact of systematic errors in more detail.

Appendix A

A1 Sensitivity tests on the *a priori* emission error and its spatial correlation length

To test the system with different choices for the *a priori* emission error and its spatial correlation length, we perform experiments S1.1 and S1.2. Results are tabulated in Table 3. In S1.1, the uncertainty of the *a priori* emissions is set to 1000% of the *a priori* emissions values, and the spatial correlation length to 10 km. In S1.2, the uncertainty

remains 300%, and the correlation length is set to 200 km. These settings imply the following. In S1.1, the system has much more degrees of freedom and can potentially deviate stronger from the *a priori* emissions with marked variation between grid cells due to the small spatial correlation length. In scenario S1.2, we may expect areas with high CH₄ emissions with values of the same order as S1, but with stronger correlation at regional scale.

Figure A1 shows the *a posteriori* annual mean CH₄ emission distributions for scenarios S1.1 and S1.2. The annual mean emission distribution derived for S1.1 has a more distinct spatial structure than S1 (e.g. for the UK, Eastern Europe, and the Benelux countries). Hot spot areas are more localized with higher values for the peaks compared to S1.

As expected, scenario S1.2 shows derived annual mean CH₄ emissions with more homogeneously distributed spatial patterns. As an effect of the larger value for the spatial correlation length, emission hot spots are distributed over wider areas (e.g. UK, Benelux, Eastern Europe), and emission peak values are smaller compared to the S1 and S1.1 scenarios.

The annual totals at the country scale presented in Table 4, show that both S1.1 and S1.2 overestimate the derived CH₄ emissions for En-EU27 (about 10%), compared to S1. The settings chosen for S1 determine annual mean CH₄ emissions closer to the true emissions (less than 5% difference for En-EU27).

A2 Sensitivity tests on the perturbations applied to synthetic observations

To assess the robustness of the *a posteriori* emissions, we tested our TM5-4DVAR system by using (i) non perturbed synthetic observations (scenario S1.3 in Table 3), and (ii) synthetic observations perturbed with random noise with amplitude equal to the measurement error of 3 ppb (scenario S1.4) instead of the 50% of the representativeness error estimated from the forward simulation.

Firstly, we analyze the amount of measurements that are rejected after the first optimization cycle. The amounts of measurements that are not used in the second cycle of

Inverse modeling of European CH₄ emissions

M. G. Villani et al.

Title Page

Abstract

Introduction

Conclusions

References

Tables

Figures

◀

▶

◀

▶

Back

Close

Full Screen / Esc

Printer-friendly Version

Interactive Discussion



the inversion are 7%, 2%, and 2% for scenarios S1, S1.3, and S1.4, respectively. This result is expected, since when measurements are not or are less strongly perturbed, the system is able to reproduce these pseudo-measurements better.

We found that the spatial patterns for the derived European annual mean emission distributions (not shown here) do not show relevant differences in the three scenarios. At the country scale, for the En-EU27 (Table 4), the total annual emissions for S1, S1.3, and S1.4 differ generally by less than 2%. This shows that the perturbation of the pseudo-measurements does not influence the results significantly.

Acknowledgements. This work has been supported by the European Commission RTD project GEMS (“Global and regional Earth-system (Atmosphere) Monitoring using Satellite and in-situ data”, contract number SIP4-CT-2004-516099, 6th Framework Programme). We are grateful to Arjo Segers for his support concerning the TM5 model framework and assistance in preprocessing the ECMWF meteorological data as TM5 input. Furthermore, we would like to thank Julian Wilson for his helpful comments.

References

Bergamaschi, P., Krol, M., Dentener, F., Vermeulen, A., Meinhardt, F., Graul, R., Ramonet, M., Peters, W., and Dlugokencky, E. J.: Inverse modelling of national and European CH₄ emissions using the atmospheric zoom model TM5, *Atmos. Chem. Phys.*, 5, 2431–2460, 2005,

<http://www.atmos-chem-phys.net/5/2431/2005/>.

Bergamaschi, P. (Ed.): Atmospheric Monitoring and Inverse Modelling for Verification of National and EU Bottom-up GHG Inventories – report of the workshop “Atmospheric Monitoring and Inverse Modelling for Verification of National and EU Bottom-up GHG Inventories” under the mandate of Climate Change Committee Working Group I, Casa Don Guanella, Ispra, Italy (8–9 March 2007), European Commission Joint Research Centre, Institute for Environment and Sustainability, 153 pp., 2007a.

Bergamaschi, P., Frankenberg, C., Meirink, J. F., Krol, M., Dentener, F., Wagner, T., Platt, U., Kaplan, J. O., Körner, S., Heimann, M., Dlugokencky, E. J., and Goede, A.: Satellite cartography of atmospheric methane from SCIAMACHY onboard ENVISAT:

Inverse modeling of European CH₄ emissions

M. G. Villani et al.

Title Page

Abstract

Introduction

Conclusions

References

Tables

Figures

◀

▶

◀

▶

Back

Close

Full Screen / Esc

Printer-friendly Version

Interactive Discussion



- (II) Evaluation based on inverse model simulations, *J. Geophys. Res.*, 112, D02304, doi:02310.01029/02006JD007268, 2007b.
- Bergamaschi, P., Frankenberg, C., Meirink, J. F., Krol, M., Villani, M. G., Houweling, S., Dentener, F., Dlugokencky, E. J., Miller, J. B., Engel, A., and Levin, I.: Inverse Modeling of global and regional CH₄ emissions using SCIAMACHY satellite retrievals, *J. Geophys. Res.-Atmos.*, accepted, 2009.
- Bousquet, P., Hauglustaine, D. A., Peylin, P., Carouge, C., and Ciais, P.: Two decades of OH variability as inferred by an inversion of atmospheric transport and chemistry of methyl chloroform, *Atmos. Chem. Phys.*, 5, 2635–2656, 2005, <http://www.atmos-chem-phys.net/5/2635/2005/>.
- Brühl, C. and P. J. Crutzen: The MPIC 2D model, in *NASA Ref. Publ.* 1292, vol. 1, 103–104, 1993.
- Carouge, C., Bousquet, P., Peylin, P., Rayner, P. J., and Ciais, P.: What can we learn from European continuous atmospheric CO₂ measurements to quantify regional fluxes – Part 1: Potential of the network, *Atmos. Chem. Phys. Discuss.*, 8, 18591–18620, 2008a, <http://www.atmos-chem-phys-discuss.net/8/18591/2008/>.
- Carouge, C., Peylin, P., Rayner, P. J., Bousquet, P., Chevallier, F., and Ciais, P.: What can we learn from European continuous atmospheric CO₂ measurements to quantify regional fluxes – Part 2: Sensitivity of flux accuracy to inverse setup, *Atmos. Chem. Phys. Discuss.*, 8, 18621–18649, 2008b, <http://www.atmos-chem-phys-discuss.net/8/18621/2008/>.
- Chen, Y.-H. and Prinn, R. G.: Estimation of atmospheric methane emissions between 1996 and 2001 using a three-dimensional global chemical transport model, *J. Geophys. Res.*, 111, D10307, doi:10310.11029/12005JD006058, 2006.
- Chevallier, F.: Impact of correlated observation errors on inverted CO₂ surface fluxes from OCO measurements, *Geophys. Res. Lett.*, 34, L24804, doi:10.1029/2007GL030463, 2007.
- Dlugokencky, E. J., Masarie, K. A., Lang, P. M., Steele, P. P., and Nisbet, E. G.: A dramatic decrease in the growth rate of atmospheric methane in the northern hemisphere during 1992, *Geophys. Res. Lett.*, 21, 45–48, 1994.
- Dlugokencky, E. J., Houweling, S., Bruhwiler, L., Masarie, K. A., Lang, P. M., Miller, J. B., and Tans, P. P.: Atmospheric methane levels off: Temporary pause or a new steady-state?, *Geophys. Res. Lett.*, 30(19), 1992, doi:1910.1029/2003GL018126, 2003.
- Frankenberg, C., Bergamaschi, P., Butz, A., Houweling, S., Meirink, J. F., Notholt, J., Pe-

**Inverse modeling of
European CH₄
emissions**M. G. Villani et al.

[Title Page](#)[Abstract](#)[Introduction](#)[Conclusions](#)[References](#)[Tables](#)[Figures](#)[◀](#)[▶](#)[◀](#)[▶](#)[Back](#)[Close](#)[Full Screen / Esc](#)[Printer-friendly Version](#)[Interactive Discussion](#)

tersen, A. K., Schrijver, H., Warneke, T., and Aben, I.: Tropical methane emissions: A revised view from SCIAMACHY onboard ENVISAT, *Geophys. Res. Lett.*, 35, L15811, doi:10.1029/2008GL034300, 2008.

Hein, R., Crutzen, P. J., and Heimann, M.: An inverse modeling approach to investigate the global atmospheric methane cycle, *Global Biogeochem. Cy.*, 11, 43–76, 1997.

Houweling, S., Dentener, F., and Lelieveld, J.: The impact of nonmethane hydrocarbon compounds on tropospheric photochemistry, *J. Geophys. Res.*, 103(D9), 10673–10696, 1988.

Houweling, S., Kaminski, T., Dentener, F., Lelieveld, J., and Heimann, M.: Inverse modeling of methane sources and sinks using the adjoint of a global transport model, *J. Geophys. Res.*, 104(D21), 26137–26160, 1999.

IPCC: Good Practice Guidance and Uncertainty Management in National Greenhouse Gas Inventories, Published for the IPCC by the Institute for Global Environmental Strategies, Japan, 2000.

Krol, M., Houweling, S., Bregman, B., van den Broek, M., Segers, A., van Velthoven, P., Peters, W., Dentener, F., and Bergamaschi, P.: The two-way nested global chemistry-transport zoom model TM5: algorithm and applications, *Atmos. Chem. Phys.*, 5, 417–432, 2005, <http://www.atmos-chem-phys.net/5/417/2005/>.

Krol, M. C., Meirink, J. F., Bergamaschi, P., Mak, J. E., Lowe, D., Jöckel, P., Houweling, S., and Röckmann, T.: What can ^{14}C measurements tell us about OH?, *Atmos. Chem. Phys.*, 8, 5033–5044, 2008, <http://www.atmos-chem-phys.net/8/5033/2008/>.

Lambert, G. and Schmidt, S.: Reevaluation of the oceanic flux of methane: Uncertainties and long term variations, *Chemosphere: Global Change Science*, 26(1–4), 579–589, 1993.

Law, R. M. and P. F. Vohralik: Methane sources from mass-balance inversions: sensitivity to transport, CSIRO Atmospheric Research Technical Paper no. 50, 27 pp., 2001.

Law, R. M., Rayner, P. J., Steele, L. P., and Enting, I. G.: Using high frequency data for CO_2 inversions, *Global Biogeochem. Cy.*, 16(4), 1053, doi:10.1029/2001GB001593, 2002.

Law, R. M., Rayner, P. J., Steele, L. P., and Enting, I. G.: Data and Modelling requirements for CO_2 inversions using high-frequency data, *Tellus*, 55B, 512–521, 2003.

Law, R. M., Rayner, P. J., and Wang, Y. P.: Inversion of diurnally varying synthetic CO_2 : Network optimization for an Australian test case, *Global Biogeochem. Cy.*, 18, GB1044, doi:10.29/2003GB002136, 2004.

Manning, M. R., Lowe, D. C., Moss, R. C., Bodeker, G. E., and Allan, W.: Short term variations

Inverse modeling of European CH_4 emissions

M. G. Villani et al.

Title Page

Abstract

Introduction

Conclusions

References

Tables

Figures

◀

▶

◀

▶

Back

Close

Full Screen / Esc

Printer-friendly Version

Interactive Discussion



**Inverse modeling of
European CH₄
emissions**

M. G. Villani et al.

Title Page

Abstract

Introduction

Conclusions

References

Tables

Figures

◀

▶

◀

▶

Back

Close

Full Screen / Esc

Printer-friendly Version

Interactive Discussion

in the oxidizing power of the atmosphere, *Nature*, 436, 1001–1004, 2005.

Matthews, E., Fung, I., and Lerner, J.: Methane emission from rice cultivation: Geographic and seasonal distribution of cultivated areas and emissions, *Global Biogeochem. Cy.*, 5, 3–24, 1991.

5 Meirink, J. F., Eskes, H. J., and Goede, A. P. H.: Sensitivity analysis of methane emissions derived from SCIAMACHY observations through inverse modelling, *Atmos. Chem. Phys.*, 6, 1275–1292, 2006,

<http://www.atmos-chem-phys.net/6/1275/2006/>.

Meirink, J. F., Bergamaschi, P., and Krol, M. C.: Four-dimensional variational data assimilation for inverse modelling of atmospheric methane emissions: method and comparison with syn-

10 thesis inversion, *Atmos. Chem. Phys.*, 8, 6341–6353, 2008a,

<http://www.atmos-chem-phys.net/8/6341/2008/>.

Meirink, J. F., Bergamaschi, P., Frankenberg, C., d'Amelio, M. T. S., Dlugokencky, E. J., Gatti, L. V., Houweling, S., Miller, J. B., Rockmann, T., Villani, M. G., and Krol, M.: Four-dimensional variational data assimilation for inverse modelling of atmospheric methane emissions: Analysis of SCIAMACHY observations, *J. Geophys. Res.*, 113, D17301, doi:10.1029/2007JD009740, 2008b.

Mikaloff Fletcher, S. E., Tans, P. P., Bruhwiler, L. M., Miller, J. B., and Heimann, M.: CH₄ sources estimated from atmospheric observations of CH₄ and its ¹³C/¹²C isotopic ratios: 2. Inverse modelling of CH₄ fluxes from geographical regions, *Global Biogeochem. Cy.*, 18, GB4005, doi:10.1029/2004GB002224, 2004a.

20 Mikaloff Fletcher, S. E., Tans, P. P., Bruhwiler, L. M., Miller, J. B., and Heimann, M.: CH₄ sources estimated from atmospheric observations of CH₄ and its ¹³C/¹²C isotopic ratios: 1. Inverse modelling of source processes, *Global Biogeochem. Cy.*, 18, GB4009, doi:10.1029/2004GB002223, 2004b.

Olivier, J. G. J. and Berdowski, J. J. M.: Global emissions sources and sinks, in: *The climate system*, edited by: Berdowski, J. J. M., Guicherit, R., and Heij, J. B., A.A. Balkema Publishers/Swets & Zeitlinger Publishers, Lisse, The Netherlands, 2001.

Prinn, R., Cunnold, D., Rasmussen, R., Simmonds, P., Alyea, F., Crawford, A., Fraser, P., and Rosen, R.: Atmospheric Emissions and Trends of Nitrous Oxide Deduced From 10 Years of ALE-GAGE Data, *J. Geophys. Res.*, 95(D11), 18369–18385, 1990.

30 Rayner, P. J., Enting, I. G., and Trudinger, C. M.: Optimizing the CO₂ observing Network for constraining sources and sinks, *Tellus*, 48B, 433–444, 1996.



Ridgwell, A. J., Marshall, S. J., and Gregson, K.: Consumption of atmospheric methane by soils: A process-based model, *Global Biogeochem. Cy.*, 13(1), 59–70, doi:10.1029/1998GB900004, 1999.

Sanderson, M. G.: Biomass of termites and their emissions of methane and carbon dioxide: A global database, *Global Biogeochem. Cy.*, 10, 543–557, 1996.

van der Werf, G. R., Randerson, J. T., Collatz, G. J., Giglio, L., Kasibhatla, P. S., Arellano Jr., A. F., Olsen, S. C., and Kasischke, E. S.: Continental-Scale Partitioning of Fire Emissions During the 1997 to 2001 El Nino/LaNina Period, *Science*, 303, 73–76, 2004.

ACPD

9, 21073–21110, 2009

Inverse modeling of European CH₄ emissions

M. G. Villani et al.

Title Page

Abstract

Introduction

Conclusions

References

Tables

Figures

◀

▶

◀

▶

Back

Close

Full Screen / Esc

Printer-friendly Version

Interactive Discussion



Inverse modeling of European CH₄ emissions

M. G. Villani et al.

Title Page

Abstract

Introduction

Conclusions

References

Tables

Figures

◀

▶

◀

▶

Back

Close

Full Screen / Esc

Printer-friendly Version

Interactive Discussion



Table 1. Bottom-up emission inventories used to generate the synthetic observations.

source category	Reference	emission [Tg CH ₄ /yr]
“wetlands and rice”		
wetlands	“JK” inventory [Bergamaschi et al., 2007b] ^a	174.9
rice	GISS [Matthews et al., 1991]	59.7
“biomass burning”		
biomass burning	GFEDv2 [van der Werf et al., 2004]	20.1
“remaining sources”		
coal mining	EDGARv3.2FT [Olivier and Berdowski, 2001] ^b	33.2
oil production, transmission and handling	EDGARv3.2FT [Olivier and Berdowski, 2001] ^b	10.4
gas production and transmission	EDGARv3.2FT [Olivier and Berdowski, 2001] ^b	48.7
fossil fuel use	EDGARv3.2FT [Olivier and Berdowski, 2001] ^b	3.4
industrial processes	EDGARv3.2FT [Olivier and Berdowski, 2001] ^b	0.9
bio fuel	EDGARv3.2FT [Olivier and Berdowski, 2001] ^b	14.9
enteric fermentation	EDGARv3.2FT [Olivier and Berdowski, 2001] ^b	80.4
animal waste management	EDGARv3.2FT [Olivier and Berdowski, 2001] ^b	8.5
waste handling	EDGARv3.2FT [Olivier and Berdowski, 2001] ^b	58.1
wild animals	[Houweling et al., 1999]	5.0
termites	[Sanderson, 1996]	19.4
ocean	[Houweling et al., 1999; Lambert and Schmidt, 1993]	17.0
soil sink	[Ridgwell et al., 1999]	–38.0
total		516.5

^areference year 2000;

^b3-months running mean applied.

Table 2. List of the stations used in the synthetic experiments. Global flask measurement sites are named “RM”. Over Europe the current observational network stations are denoted as “CS”. The sites added to the CS network to form the extended network are called “EXT”. Latitudes and longitudes are expressed in degrees. Altitudes are in meters. Sites are with continuous (CM) or flask (FM) measurements. Symbols “DY” and “NI” define daytime and nighttime sampling, respectively.

Inverse modeling of European CH₄ emissions

M. G. Villani et al.

ID_OBS	O.N.	STATIONNAME	LAT	LON	ALT	TP	time
ALT	RM	Alert. Nunavut. Canada	82.45	-62.52	210	FM	DY
ZEP	CS	Ny-Alesund. Svalbard (Spitsbergen). Norway and Sweden	78.90	11.88	475	FM	DY
SUM	RM	Summit. Greenland	72.58	-38.48	3238	FM	DY
BRW	RM	Barrow. Alaska. USA	71.32	-156.60	11	FM	DY
PAL	EXT	Pallas. Finland	67.97	24.12	560	CM	DY
STM	CS	Ocean station M. Norway	66.00	2.00	5	FM	DY
TRH	EXT	Trondheim airport. Norway	63.46	10.93	15	CM	DY
ICE	CS	Heimay. Vestmannaeyjar. Iceland	63.34	-20.29	127	FM	DY
BNR	EXT	Bergen Airport. Norway	60.30	5.24	100	CM	DY
HEL	EXT	Helsinki Airport. Sweden	60.24	24.96	51	CM	DY
OSL	EXT	Oslo Airport. Norway	60.19	11.10	215	CM	DY
NRD	EXT	Norunda. Sweden	60.08	17.47	147	CM	DY
SIS	RM	Shetland Island. UK	60.08	-1.25	30	FM	DY
VKV	EXT	Voeikovo. St Petersburg. Russia	59.95	30.70	72	CM	DY
RIG	EXT	Riga. Latvia	56.92	23.98	20	CM	DY
TT1	EXT	Angus. UK	56.55	-2.98	535	CM	DY
BAL	RM	Baltic Sea. Poland	55.35	17.22	28	FM	DY
CBA	RM	Cold Bay. Alaska. USA	55.20	-162.70	25	FM	DY
WES	EXT	Westerland. Germany	54.93	8.32	12	CM	DY
ZGT	EXT	Zingst. Germany	54.44	12.72	1	CM	DY
DAZ	EXT	Danzica. Poland	54.35	18.63	28	CM	DY
MHD	CS	Mace Head. Ireland	53.33	-9.90	25	CM	DY
SHM	RM	Shemya Island. Alaska. USA	52.72	174.10	40	FM	DY
NTW	EXT	Newtown. Wales	52.52	-3.32	294	CM	DY
PZN	EXT	Pozna airport. Poland	52.42	16.84	100	CM	DY
BI5	EXT	Bialystok. Poland	52.25	22.75	460	CM	DY
CB4	CS	Cabauw. Netherlands	51.97	4.93	200	CM	DY
LON	CS	Royal Holloway. University of London. UK	51.43	-0.56	45	CM	DY
KIV	EXT	Kiev airport. Ucraina	50.42	30.52	162	CM	DY
PRG	EXT	Prague airport. Czech Republic	50.09	14.37	280	CM	DY
KRK	EXT	Krakow. University of Mining and Metallurgy. Poland	50.07	19.92	215	CM	DY
OX3	EXT	Ochsenkopf. Germany	50.05	11.82	1185	CM	DY
DEU	EXT	Deusselbach. Germany	49.76	7.05	480	CM	DY
HDB	EXT	Heidelberg. Germany	49.40	8.70	136	CM	DY

Title Page

Abstract

Introduction

Conclusions

References

Tables

Figures

◀

▶

◀

▶

Back

Close

Full Screen / Esc

Printer-friendly Version

Interactive Discussion



Table 2. Continued.

ID_OBS	O.N.	STATIONNAME	LAT	LON	ALT	TP	time
KPW	EXT	Kasprowy Wierch. Poland/Slovakia	49.23	19.93	1987	CM	NI
ILE	EXT	Ile Grande. France	48.81	-3.57	5	FM	DY
GIF	CS	Saclay. France	48.72	2.15	20	CM	DY
ORL	EXT	Orleans. Trainou. France	47.95	2.10	311	CM	DY
SIL	CS	Schauinsland. Germany	47.91	7.91	1205	CM	NI
HPB	EXT	Hohenpeissenberg. Germany	47.78	11.00	990	FM	DY
ZUG	CS	Zugspitze. Germany	47.42	10.98	2960	CM	NI
HU1	CS	Hegyhatsal. Hungary	46.95	16.65	344	FM	DY
CLJ	EXT	Cluj Airport. Romania	46.78	23.65	400	CM	DY
JFJ	EXT	Jungfrauoch. Switzerland	46.55	7.98	3580	CM	NI
ISP	EXT	Ispra (VA). Italy	45.80	8.63	209	CM	DY
ORS	EXT	Mt Orsa (VA). Italy	45.89	8.91	1015	CM	DY
ZAG	EXT	Zagreb Airport. Croatia	45.77	16.01	120	CM	DY
PUY	CS	Puy de Dome. France	45.77	2.97	1465	FM	NI
QUI	EXT	Quistello (Mantova). Italia	45.01	10.98	200	CM	DY
BRD	EXT	Bordeaux Airport. France	44.83	-0.70	52	CM	DY
SPC	EXT	San Pietro Capofiume. Italy	44.65	11.62	211	CM	DY
KZD	RM	Sary Taukum. Kazakhstan	44.45	75.57	412	FM	DY
UUM	RM	Ulaan Uul. Mongolia	44.45	111.10	914	FM	DY
CMN	EXT	Monte Cimone. Italy	44.17	10.68	2165	CM	NI
BSC	CS	Black Sea. Constanta. Romania	44.17	28.68	3	FM	DY
SRJ	EXT	Sarajevo (airport)	43.83	18.34	507	CM	DY
MRS	EXT	Marseille Airport. France	43.35	5.50	400	CM	DY
KZM	RM	Plateu Assy. Kazakhstan	43.25	77.88	2519	FM	DY
PDM	CS	Pic du Midi. France	42.94	0.14	2877	FM	NI
SOF	EXT	Sofia (airport). Bulgaria	42.69	23.40	535	CM	DY
BGU	CS	Begur. Spain	41.97	3.23	13	FM	DY
RCC	EXT	Roccaraso. L'Aquila. Italy	41.84	14.08	1400	CM	NI
RMP	EXT	Rome Pomezia. Italy	41.67	12.50	100	CM	DY
MUE	EXT	La Muela. Spain	41.58	-1.83	200	CM	DY
TIR	EXT	Tirana (airport). Albania	41.42	19.71	32	CM	DY
AVR	EXT	Aveiro. Portugal	40.64	-8.65	10	FM	DY
IMA	EXT	IMAA (PZ) Italy	40.60	15.72	800	CM	DY
NWR	RM	Niwot Ridge. Colorado. USA	40.05	-105.60	3526	FM	NI
ORI	EXT	Oristano (Italy) IMC	39.90	8.60	11	CM	DY
UTA	RM	Wendover. Utah. USA	39.90	-113.70	1320	FM	DY
VAL	EXT	Valencia Airport. Spain	39.49	-0.48	63	CM	DY
PTA	RM	Point Arena. California. USA	38.95	-123.70	17	FM	DY
AZR	RM	Terceira Island. Azores. Portugal	38.77	-27.38	40	FM	DY

Inverse modeling of European CH₄ emissions

M. G. Villani et al.

Title Page

Abstract Introduction

Conclusions References

Tables Figures

◀ ▶

◀ ▶

Back Close

Full Screen / Esc

Printer-friendly Version

Interactive Discussion



Table 2. Continued.

ID_OBS	O.N.	STATIONNAME	LAT	LON	ALT	TP	time
ATH	EXT	Athens Airport. Greece	37.95	23.87	200	CM	DY
SEV	EXT	Sevilla Airport. Spain	37.42	-5.90	36	CM	DY
ENN	EXT	Enna (Italy). Interbus (spa). Italy	37.57	14.28	870	CM	DY
TAP	RM	Tae-ahn Peninsula. Republic of Korea	36.73	126.10	20	FM	DY
WLG	RM	Mt. Waliguan. Peoples Republic of China	36.29	100.90	3810	FM	NI
LMP	CS	Lampedusa. Italy	35.52	12.63	45	FM	DY
FKL	EXT	Finokalia. Crete. Greece	35.33	25.67	250	FM	DY
TRO	EXT	Troodos. Cyprus	35.03	33.05	520	FM	DY
BME	RM	St. Davis Head. Bermuda. UK	32.37	-64.65	30	FM	DY
BMW	RM	Tudor Hill. Bermuda. UK	32.27	-64.88	30	FM	DY
WIS	CS	Sede Boker. Negev Desert. Israel	31.13	34.88	400	FM	DY
IZO	CS	Tenerife. Canary Islands. Spain	28.30	-16.48	2360	FM	NI
MID	RM	Sand Island. Midway. USA	28.21	-177.40	8	FM	DY
KEY	RM	Key Biscayne. Florida. USA	25.67	-80.20	3	FM	DY
ASK	RM	Assekrem. Algeria	23.18	5.42	2728	FM	NI
MLO	RM	Mauna Loa. Hawaii. USA	19.53	-155.60	3397	FM	NI
KUM	RM	Cape Kumukahi. Hawaii. USA	19.52	-154.80	3	FM	DY
GMI	RM	Mariana Islands. Guam	13.43	144.80	6	FM	DY
RPB	RM	Ragged Point. Barbados	13.17	-59.43	45	FM	DY
CHR	RM	Christmas Island. Republic of Kiribati	1.70	-157.20	3	FM	DY
SEY	RM	Mahe Island. Seychelles	-4.67	55.17	7	FM	DY
ASC	RM	Ascension Island. UK	-7.92	-14.42	54	FM	DY
SMO	RM	Tutuila. American Samoa. USA	-14.24	-170.60	42	FM	DY
EIC	RM	Easter Island. Chile	-27.15	-109.50	50	FM	DY
CGO	RM	Cape Grim. Tasmania. Australia	-40.68	144.70	94	FM	DY
CRZ	RM	Crozet Island. France	-46.45	51.85	120	FM	DY
TDF	RM	Tierra Del Fuego. La Redonda Isla. Argentina	-54.87	-68.48	20	FM	DY
PSA	RM	Palmer Station. Antarctica. USA	-64.92	-64.00	10	FM	DY
SYO	RM	Syowa Station. Antarctica. Japan	-69.00	39.58	14	FM	DY
HBA	RM	Halley Station. Antarctica. UK	-75.58	-26.50	33	FM	DY
SPO	RM	South Pole. Antarctica. USA	-89.98	-24.80	2810	FM	DY

Inverse modeling of European CH₄ emissions

M. G. Villani et al.

Title Page

Abstract

Introduction

Conclusions

References

Tables

Figures

◀

▶

◀

▶

Back

Close

Full Screen / Esc

Printer-friendly Version

Interactive Discussion



Inverse modeling of European CH₄ emissions

M. G. Villani et al.

Table 3. List of the sensitivity tests discussed in this work.

Inversion	Network	<i>a priori</i> uncertainty	Lc spatial correlation length	Perturbation syn. obs.	Description
Inversions for Single stations					
I1	MHD	300%	50 km	50% repr. error	footprint an inversion of MHD
I2	CB4	300%	50 km	50% repr. error	footprint an inversion of CB4
I3	SIL	300%	50 km	50% repr. error	footprint an inversion of SIL
Inversions for Observational Networks					
S1	CS	300%	50 km	50% repr. error	inversion for CS
S2	CS-CM	300%	50 km	50% repr. error	inversion for CS-CM
S3	EXT	300%	50 km	50% repr. error	inversion for EXT
Inversions for observational Networks with no CH ₄ emissions from Ocean					
S1.a	CS	300%	50 km	no perturbation	inversion for CS
S2.a	CS-CM	300%	50 km	no perturbation	inversion for CS-CM
S3.a	EXT	300%	50 km	no perturbation	inversion for EXT
LINEAR Inversions for observational Networks with no CH ₄ emissions from Ocean					
S1.b	CS	300%	50 km	no perturbation	inversion for CS
S2.b	CS-CM	300%	50 km	no perturbation	inversion for CS-CM
S3.b	EXT	300%	50 km	no perturbation	inversion for EXT
Appendix: sensitivity to inversion parameters					
S1.1	CS	1000%	10 km	50% repr. error	sensitivity to <i>a priori</i> uncertainty
S1.2	CS	300%	200 km	50% repr. error	sensitivity to correlation length
S1.3	CS	300%	50 km	no perturbation	sensitivity to syn.obs. not perturbed
S1.4	CS	300%	50 km	3 ppb	sensitivity to syn.obs. perturbed

Title Page

Abstract

Introduction

Conclusions

References

Tables

Figures

◀

▶

◀

▶

Back

Close

Full Screen / Esc

Printer-friendly Version

Interactive Discussion



Inverse modeling of
European CH₄
emissions

M. G. Villani et al.

Table 4. Annual total methane emissions for European countries (units in Tg CH₄/yr).

ID	Countries	TRUE	APRI	S1	S1.a	S1.b	S2	S2.a	S2.b	S3	S3.a	S3.b	S1.1	S1.2	S1.3	S1.4
Gbout ¹	offshore	0.54	0.01	0.01	0.00	0.00	0.01	0.00	0.00	0.02	0.00	0.00	0.01	0.03	0.01	0.01
NO	Norway	0.86	1.03	1.22	0.90	0.87	0.91	0.78	0.74	1.27	1.03	0.99	1.22	1.19	1.07	1.08
SE	Sweden	0.92	1.63	1.45	1.33	1.26	1.19	1.08	0.96	0.98	1.01	0.92	1.49	1.09	1.36	1.46
FI	Finland	0.61	1.24	1.03	1.00	0.98	1.03	0.88	0.84	0.80	0.75	0.67	1.08	0.95	0.98	1.04
LV+LT+ET	Latvia Lithuania Estonia	0.31	0.62	0.67	0.64	0.68	0.50	0.51	0.48	0.41	0.33	0.24	0.64	0.63	0.66	0.66
UK+IRL	UK Ireland	3.31	1.09	2.99	3.02	3.04	3.59	3.18	3.20	3.49	3.21	3.16	3.24	3.52	3.24	3.25
BENELUX	Benelux	1.21	0.20	1.30	1.30	1.28	1.28	1.36	1.35	1.33	1.33	1.33	1.35	1.38	1.32	1.32
DA	Denmark	0.28	0.12	0.29	0.21	0.22	0.27	0.29	0.31	0.34	0.31	0.31	0.35	0.42	0.23	0.23
FR	France	2.41	2.06	2.88	2.77	2.63	2.66	2.69	2.59	2.52	2.49	2.40	3.01	2.87	2.72	2.70
DE	Germany	3.54	1.34	3.41	3.63	3.64	3.33	3.36	3.40	3.47	3.57	3.59	3.58	3.68	3.53	3.45
AT	Austria	0.34	0.31	0.43	0.37	0.35	0.52	0.47	0.45	0.36	0.34	0.33	0.39	0.38	0.41	0.41
CH	Switzerland	0.16	0.15	0.19	0.18	0.18	0.16	0.18	0.18	0.14	0.10	0.06	0.18	0.19	0.19	0.20
PL	Poland	3.22	1.19	2.46	2.33	2.36	2.65	2.79	2.83	3.48	3.57	3.36	2.66	3.04	2.39	2.45
HU	Hungary	0.51	0.36	0.56	0.52	0.53	0.56	0.50	0.46	0.32	0.27	0.34	0.58	0.73	0.55	0.56
CS+SL	Czech rep. Slovakia	1.02	0.47	1.11	1.12	1.13	1.32	1.38	1.38	1.38	1.42	1.26	1.32	1.42	1.09	1.12
BG	Bulgaria	0.31	0.42	0.41	0.39	0.39	0.42	0.39	0.37	0.46	0.43	0.43	0.40	0.39	0.40	0.41
RO	Romania	1.23	0.89	1.19	1.13	1.16	1.46	1.44	1.46	1.55	1.48	1.41	1.21	1.11	1.15	1.19
Ex Yug.	Former Yugoslavia	0.74	0.97	0.99	0.94	0.99	1.17	1.03	0.98	0.98	0.95	0.87	1.00	0.88	0.98	1.02
ES+PT	Spain Portugal	1.67	1.87	1.77	1.67	1.65	1.82	1.73	1.69	1.83	1.68	1.62	1.74	1.84	1.70	1.74
IT	Italy	2.01	1.11	1.61	1.40	1.40	1.61	1.54	1.54	2.26	2.37	2.05	1.68	1.71	1.47	1.52
GR+MT+CY	Greece Malta Cyprus	0.37	0.46	0.44	0.41	0.43	0.39	0.35	0.33	0.41	0.37	0.32	0.45	0.40	0.43	0.44
NWE ²	North West Countries	10.47	4.68	10.58	10.71	10.59	10.87	10.60	10.53	10.81	10.59	10.47	11.19	11.45	10.81	10.71
EU15	EU-15	16.98	11.73	17.90	17.43	17.20	18.01	17.25	16.95	18.08	17.71	17.00	18.67	18.61	17.69	17.88
En-EU27	Enlarged EU27	25.34	17.85	26.71	25.61	25.51	27.18	26.28	25.86	28.08	27.33	25.97	27.91	28.22	26.19	26.60
N.C. ³	North Countries	2.97	4.64	4.66	4.09	4.00	3.91	3.54	3.33	3.79	3.43	3.13	4.78	4.28	4.30	4.46
E.C. ⁴	East Countries	7.02	4.29	6.71	6.43	6.57	7.56	7.53	7.49	8.17	8.13	7.67	7.17	7.58	6.56	6.76
S.C. ⁵	South Countries	4.38	3.77	4.16	3.82	3.83	4.16	3.95	3.88	4.81	4.73	4.31	4.20	4.35	3.92	4.05

¹ Area over the North Sea (0°–5° E lon, and 54°–62° N lat) where anthropogenic emissions are located.² North West European countries (UK, IRL, FR, DE and the Benelux).³ Northern European countries (NO, SE, FI, DA, LV+LT+ET).⁴ Eastern European countries (PL, HU, CS+SL, BG, RO, Ex.Y).⁵ Southern European Countries (ES+PT, IT, GR+MT+CY).

Title Page

Abstract

Introduction

Conclusions

References

Tables

Figures

◀

▶

◀

▶

Back

Close

Full Screen / Esc

Printer-friendly Version

Interactive Discussion



Table 5. Pearson correlation coefficients (r) and linear regression coefficients ($\text{emiss}_{\text{mod}} = b * \text{emiss}_{\text{true}} + \text{offset}$) calculated for inland pixels in enlarged EU27.

Inversion	r	b	Offset ($\text{mgCH}_4/\text{m}^2/\text{day}$)
apriori	0	0	10.44
Inversions for Observational Networks			
S1	0.47	0.25	11.68
S2	0.57	0.33	10.01
S3	0.74	0.74	5.54
Inversions for observational Networks with no CH_4 emissions from Ocean			
S1.a	0.50	0.29	11.05
S2.a	0.61	0.39	9.46
S3.a	0.76	0.89	3.28
LINEAR Inversions for observational Networks with no CH_4 emissions from Ocean			
S1.b	0.45	0.30	10.71
S2.b	0.56	0.42	8.90
S3.b	0.65	0.92	1.84
Appendix: sensitivity to inversion parameters			
S1.1	0.43	0.28	11.67
S1.2	0.50	0.31	10.80
S1.3	0.51	0.26	11.36
S1.4	0.52	0.27	11.37

Inverse modeling of European CH_4 emissions

M. G. Villani et al.

Title Page

Abstract

Introduction

Conclusions

References

Tables

Figures

◀

▶

◀

▶

Back

Close

Full Screen / Esc

Printer-friendly Version

Interactive Discussion



Inverse modeling of European CH₄ emissions

M. G. Villani et al.

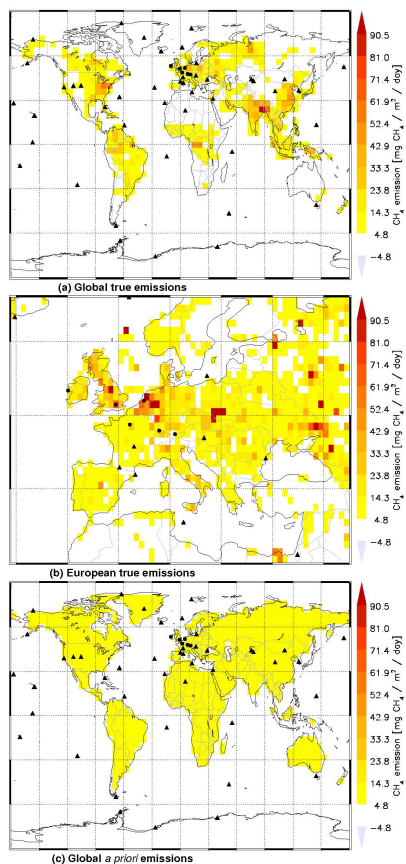


Fig. 2. Annual mean methane emission distributions: global true methane emission distribution (a), European true methane emission distribution (b), and global *a priori* emissions distribution (c). Black dots (CM sampling) and triangles (FM sampling) are the station locations for CS network.

Title Page

Abstract

Introduction

Conclusions

References

Tables

Figures

◀

▶

◀

▶

Back

Close

Full Screen / Esc

Printer-friendly Version

Interactive Discussion



Inverse modeling of
European CH₄
emissions

M. G. Villani et al.

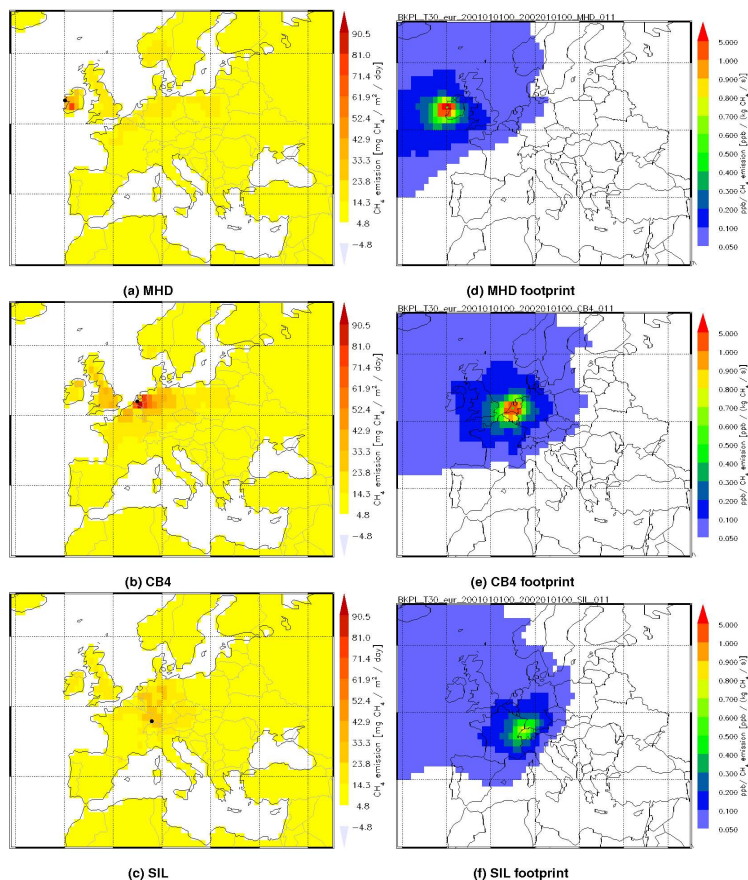


Fig. 3. Annual mean methane emission distributions and back-plume calculations calculated for scenarios I1, I2, and I3. Derived emission distributions for I1 (a); I2 (b) and I3 (c) (units are [mg CH₄/m²/day]). Back-plume calculated for I1 (d), I2 (e), and I3 (f) (units are [ppb/kg CH₄/s]).

Title Page

Abstract

Introduction

Conclusions

References

Tables

Figures

◀

▶

◀

▶

Back

Close

Full Screen / Esc

Printer-friendly Version

Interactive Discussion



Inverse modeling of
European CH₄
emissions

M. G. Villani et al.

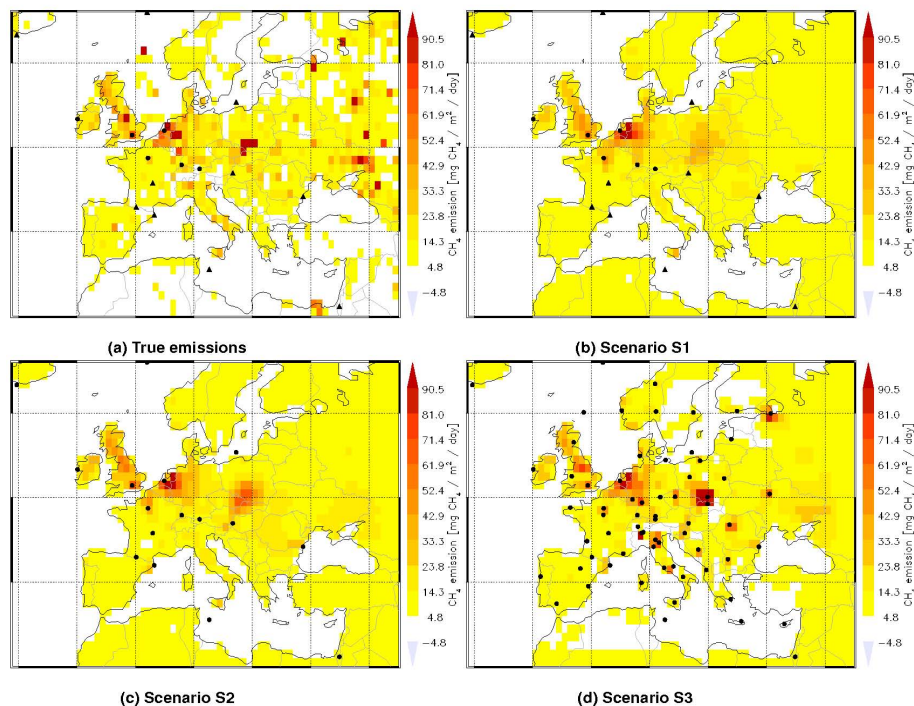


Fig. 4. Annual mean methane emission distribution for true methane emissions **(a)**; reference scenario S1 **(b)**; scenario S2 **(c)**; and S3 scenario **(d)**. Black dots (CM sampling) and triangles (FM sampling) are the station locations for different networks: CS for S1, CS-CM for S2, and EXT for S3.

[Title Page](#)[Abstract](#)[Introduction](#)[Conclusions](#)[References](#)[Tables](#)[Figures](#)[◀](#)[▶](#)[◀](#)[▶](#)[Back](#)[Close](#)[Full Screen / Esc](#)[Printer-friendly Version](#)[Interactive Discussion](#)

Inverse modeling of European CH₄ emissions

M. G. Villani et al.

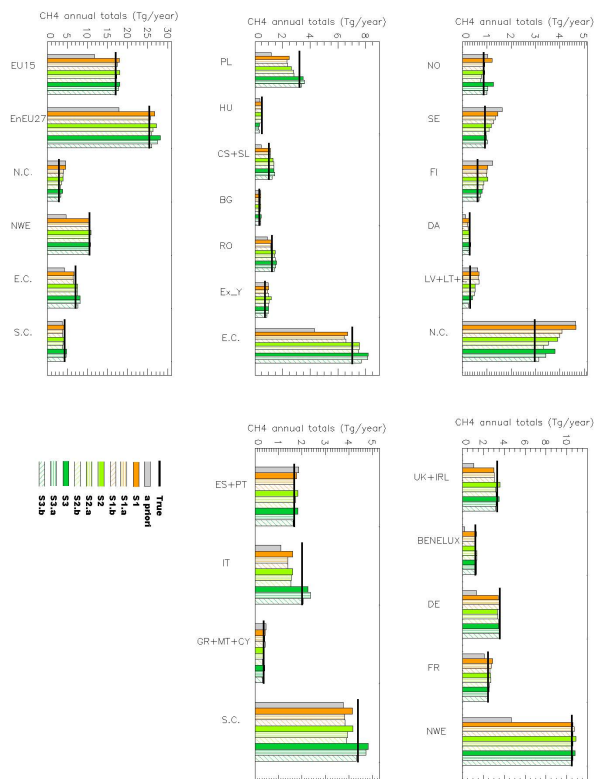


Fig. 5. Total annual emissions for selected EU countries. Horizontal bars represent the true value; grey vertical bars are the *a priori* values for each country. Colored vertical bars represent annual total emissions for scenarios in Table 4. Orange: solid is S1, vertical line pattern is S1.a, hatched pattern is S1.b. Light green: solid is S2, vertical line pattern is S2.a, hatched pattern is S2.b. Dark green: solid is S3, vertical line pattern is S3.a, hatched pattern is S3.b. Countries abbreviations are as in Table 4.

Title Page

Abstract

Introduction

Conclusions

References

Tables

Figures

◀

▶

◀

▶

Back

Close

Full Screen / Esc

Printer-friendly Version

Interactive Discussion



Inverse modeling of
European CH₄
emissions

M. G. Villani et al.

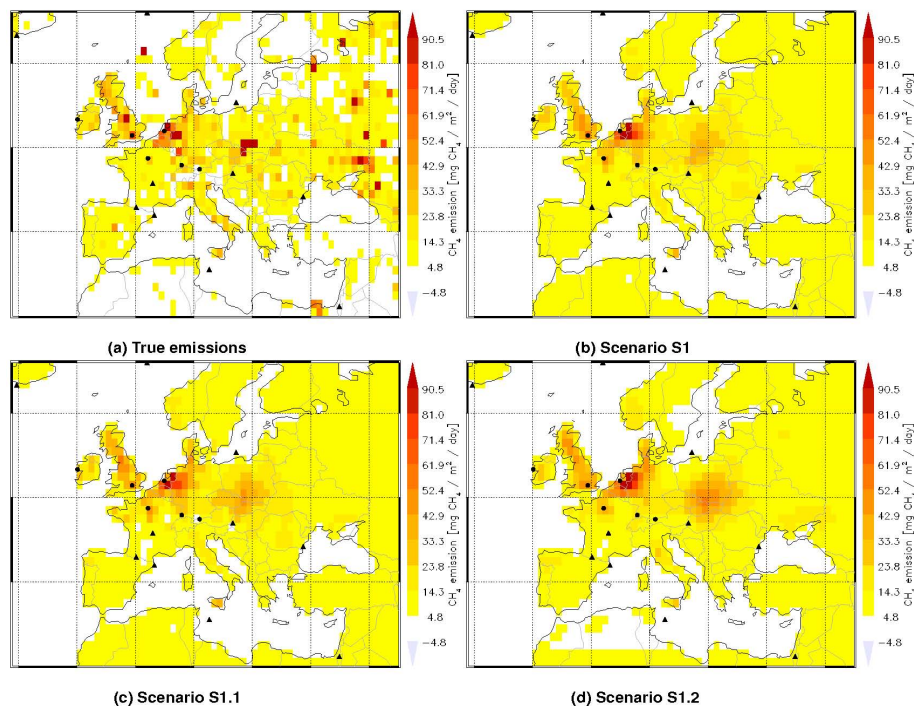


Fig. A1. Annual mean methane emission distribution for true methane emissions **(a)**; Reference scenario S1 **(b)**; scenario S1.1 **(c)**; and S1.2 scenario **(d)**. Black dots (CM sampling) and triangles (FM sampling) are the station locations for CS network.

[Title Page](#)[Abstract](#)[Introduction](#)[Conclusions](#)[References](#)[Tables](#)[Figures](#)[◀](#)[▶](#)[◀](#)[▶](#)[Back](#)[Close](#)[Full Screen / Esc](#)[Printer-friendly Version](#)[Interactive Discussion](#)